NASA TECHNICAL NOTE

NASA-TN-D-3910

NASA TN D-3910

A SIMULATOR AND FLIGHT STUDY OF YAW COUPLING IN TURNING MANEUVERS OF LARGE TRANSPORT AIRCRAFT

by Walter E. McNeill and Robert C. Innis

Ames Research Center
Moffett Field, Calif.

NATIONAL AERONAUTICS AND SPACE ADMINISTRATION • WASHINGTON, D. C. • MAY 1967

NASA TN D-3910

A SIMULATOR AND FLIGHT STUDY OF YAW COUPLING IN TURNING MANEUVERS OF LARGE TRANSPORT AIRCRAFT

By Walter E. McNeill and Robert C. Innis

Ames Research Center
Moffett Field, Calif.

NATIONAL AERONAUTICS AND SPACE ADMINISTRATION

For sale by the Clearinghouse for Federal Scientific and Technical Information
Springfield, Virginia 22151 – CFSTI price $3.00

A SIMULATOR AND FLIGHT STUDY OF YAW COUPLING IN TURNING MANEUVERS OF LARGE TRANSPORT AIRCRAFT

By Walter E. McNeill and Robert C. Innis
Ames Research Center

SUMMARY

A piloted simulator study was made of the effects of the aerodynamic yaw-coupling parameters (with Dutch-roll period and damping as secondary variables) on the lateral-directional handling qualities of a supersonic transport configuration at landing approach airspeed. Based on pilot opinions and measured sideslip excursions in sidestep maneuvers, the desirable combinations of the yaw-coupling derivatives tend to be more positive than is typical of current aircraft. Results of flight tests in a large variable-stability jet transport show trends similar to those of the simulator data. Some areas of minor disagreement between the simulator and flight results were traced to differences in pilot location with respect to the center of gravity and indicated that pilot consciousness of side acceleration forces can be an important factor in the handling qualities of large aircraft. The results of the present simulator study tend to support the use of the frequency ratio ω_φ/ω_d as an indicator of desirable yaw-coupling behavior.

INTRODUCTION

The problem of assuring satisfactory lateral-directional handling qualities in the design of a new class of airplane is a recurring one. For a transport airplane, this problem must be considered not only from the standpoint of operational safety but also from the standpoint of passenger and crew comfort. Recent studies of the lateral-directional characteristics of large aircraft, such as the supersonic transport, have pointed out some of the factors that affect the handling of a large airplane in the lateral-directional mode during such precision flight tasks as an instrument landing approach. Some examples of this work are given in references 1 and 2.

In addition to providing satisfactory lateral oscillatory (Dutch roll) characteristics, roll control response, and spiral characteristics, it is desirable that a minimum of sideslip be developed in rolling maneuvers, such as turn entries and reversals, in order that the rudder coordination required of the pilot be minimized. In other words, self-coordinating ("two control") qualities should be built into the airplane.

As airplanes increase in size, the provision of two-control capability at approach speeds tends to be more difficult because the moments of inertia increase much more rapidly with size than do the aerodynamic moments involved. The problem is even greater for supersonic-cruise aircraft because of the

proportionately large yawing moment of inertia associated with the long slender design. In short, any delay of the airplane's yawing into a turn causes adverse sideslip, which, in addition to generating uncomfortable side forces, can considerably impair the rolling performance if the dihedral effect is large, and can excite the Dutch-roll mode if the damping is low.

To investigate the problem of yaw coupling in a systematic manner, a piloted simulator study (including motion and a visual runway presentation) was made which involved repeated simulated ILS approaches. A SCAT 16 supersonic-transport configuration was used for the study. The principal variables in the study were yaw due to rolling, N_p, and yaw due to lateral control, N_{δ_a}, which have long been known to directly affect the yaw characteristics of airplanes. Supplementary flight data were obtained in a four-engined jet transport adapted for variable-stability testing. The experimental results of the simulator and flight studies have been summarized in reference 3. The purpose of the present report is to elaborate on the analysis of the results, to discuss the effects of N_p, N_{δ_a}, and secondary variables, such as Dutch-roll period and damping, on yaw coupling in roll maneuvers, and to present some observations on how optimum behavior may be obtained.

SYMBOLS

A_Y side acceleration sensed at cockpit, $a_Y + x_p\dot{r} + z_p\dot{p} - g \sin \varphi$, ft/sec^2

A_{Y_1}, A_{Y_2} first and second peak A_Y, ft/sec^2

a_Y lateral acceleration at center of gravity, ft/sec^2

a_Z normal acceleration at center of gravity, ft/sec^2

b wing span, swept position, ft

C_D $\frac{\text{drag}}{q_o S}$

C_L $\frac{\text{lift}}{q_o S}$

C_{L_α} $\frac{\partial C_L}{\partial \alpha}$, 1/rad

$C_{L_{\delta_e}}$ $\frac{\partial C_L}{\partial \delta_e}$, 1/rad

C_l $\quad \frac{\text{rolling moment}}{q_o S b}$

C_{l_p} $\quad \frac{\partial C_l}{\partial(pb/2V)}$, 1/rad

C_{l_r} $\quad \frac{\partial C_l}{\partial(rb/2V)}$, 1/rad

C_{l_β} $\quad \frac{\partial C_l}{\partial \beta}$, 1/rad

$C_{l_{\delta_a}}$ $\quad \frac{\partial C_l}{\partial \delta_a}$, 1/rad

$C_{l_{\delta_r}}$ $\quad \frac{\partial C_l}{\partial \delta_r}$, 1/rad

C_m $\quad \frac{\text{pitching moment}}{q_o S \bar{c}}$

C_{m_q} $\quad \frac{\partial C_m}{\partial(q\bar{c}/2V)}$, 1/rad

C_{m_α} $\quad \frac{\partial C_m}{\partial \alpha}$, 1/rad

$C_{m_{\delta_e}}$ $\quad \frac{\partial C_m}{\partial \delta_e}$, 1/rad

C_n $\quad \frac{\text{yawing moment}}{q_o S b}$

C_{n_p} $\quad \frac{\partial C_n}{\partial(pb/2V)}$, 1/rad

C_{n_r} $\quad \frac{\partial C_n}{\partial(rb/2V)}$, 1/rad

C_{n_β} $\quad \frac{\partial C_n}{\partial \beta}$, 1/rad

$C_{n_{\delta_a}}$ $\quad \frac{\partial C_n}{\partial \delta_a}$, 1/rad

$C_{n_{\delta_r}}$ $\quad \frac{\partial C_n}{\partial \delta_r}$, 1/rad

C_Y $\quad \frac{\text{side force}}{q_o S}$

C_{Y_β} $\quad \frac{\partial C_Y}{\partial \beta}$, 1/rad

$\bar{c}$ wing mean aerodynamic chord, swept position, ft

g acceleration due to gravity, ft/sec^2

h altitude, ft

I_X rolling moment of inertia, slug-ft^2

I_Y pitching moment of inertia, slug-ft^2

I_Z yawing moment of inertia, slug-ft^2

I_{XZ} product of inertia, $\frac{1}{2}(I_Z - I_X)\tan 2\epsilon$, slug-ft^2

L_β $\quad \frac{q_o S b C_{l_\beta}}{I_X}$, 1/sec^2

L_p $\quad \frac{b}{2V} \frac{q_o S b C_{l_p}}{I_X}$, 1/sec

L_r $\quad \frac{b}{2V} \frac{q_o S b C_{l_r}}{I_X}$, 1/sec

L_{δ_a} $\quad \frac{q_o S b C_{l_{\delta_a}}}{I_X}$, 1/sec^2

L_{δ_r} $\quad \frac{q_o S b C_{l_{\delta_r}}}{I_X}$, 1/sec^2

m airplane mass, slugs

N_p $\frac{b}{2V}\frac{q_o S b C_{n_p}}{I_Z}$, 1/sec

N_r $\frac{b}{2V}\frac{q_o S b C_{n_r}}{I_Z}$, 1/sec

N_β $\frac{q_o S b C_{n_\beta}}{I_Z}$, $1/sec^2$

N_{δ_a} $\frac{q_o S b C_{n_{\delta_a}}}{I_Z}$, $1/sec^2$

N_{δ_r} $\frac{q_o S b C_{n_{\delta_r}}}{I_Z}$, $1/sec^2$

P Dutch-roll oscillation period, sec

p rolling angular velocity, rad/sec

q pitching angular velocity, rad/sec

q_o dynamic pressure, $\frac{1}{2}\rho V^2$, lb/ft^2

r yawing angular velocity, rad/sec

S wing reference area, swept position, ft^2

T thrust, lb

t time, sec

V true airspeed, ft/sec

W weight of airplane, lb

x_p cockpit distance forward of center of gravity, ft

Y_β $\frac{q_o S C_{Y_\beta}}{m}$, ft/sec^2

z_p cockpit distance above center of gravity, ft

α angle of attack, deg or rad

β sideslip angle, deg or rad

β_1 first peak sideslip angle, deg

β_2 second peak sideslip angle, deg

γ inclination of flight path with respect to horizontal, positive for climb, rad

δ_a aileron deflection, positive right-hand trailing edge down, deg or rad

δ_e elevator deflection, positive trailing edge down, deg or rad

δ_r rudder deflection, positive trailing edge left, deg or rad

ϵ angular displacement of longitudinal principal axis below body reference axis at nose, deg

ζ_d Dutch-roll damping ratio

θ pitch angle, deg or rad

λ ground track angle with respect to runway center-line extension, rad

Λ_{LE} wing leading-edge sweep angle, deg

ρ air density, slugs/ft^3

τ_R single degree-of-freedom roll time constant, $-\frac{1}{L_p}$, sec

φ bank angle, deg or rad

φ_1 first peak bank angle, deg

φ_2 second peak bank angle, deg

$\frac{|\varphi|}{|\beta|}$ ratio of bank-angle amplitude to sideslip amplitude in the Dutch-roll mode

ψ yaw angle, deg or rad

ω_d undamped natural frequency of the Dutch-roll mode, rad/sec

ω_φ undamped natural frequency appearing in the numerator quadratic of the $\frac{\varphi}{\delta_a}$ transfer function, rad/sec

$(\dot{})$ $\frac{d(\ )}{dt}$

EQUIPMENT

Motion Simulator

The Ames five-degree-of-freedom motion simulator was used in the present study (fig. 1). The simulator was used essentially as described in reference 4, that is, with the cockpit facing outward and with the lateral acceleration cues provided by centrifuge arm motion. The pilot was subjected to pitch and yaw angular motions which approximated those of the simulated airplane. (Roll motions were attenuated to 25 percent of the computed values to avoid unrealistic side forces on the pilot caused by the cab tilting.) To avoid exceeding the motion capabilities of the simulator cab and also to avoid spurious longitudinal acceleration cues due to large angular velocity of the centrifuge arm around the track, washouts were applied to all cab angular rates and displacements and to the arm acceleration and rate. The vertical motion capability of the simulator was not used.

Cockpit

The cockpit controls and panel instruments essential to the simulation were similar to those in conventional transport aircraft, except that a three-axis attitude indicator replaced the flight director. Figure 2 shows the arrangement of the cockpit. The controls consisted of a yoke and wheel, rudder pedals, and two throttles (each controlling the two engines on one side of the airplane). The panel display included the following indicators: angle of attack, sideslip, airspeed, airplane attitude (three-axis ball which also presented ILS deviation information), heading, altitude, vertical speed, engine percent rpm, control deflections, and a clock.

A televised image of a runway model with motions reproduced as described in reference 5 was used in the visual portions of the test runs. In the present study, because of limited space in the simulator cab, the image was shown on an 8-inch television tube above the instrument panel.

Analog Simulation

Simulator motion and instrument drive signals were obtained from a six-degree-of-freedom analog simulation. The airplane equations of motion (employing moments in body axes and forces in wind axes) and the necessary angle conversion formulas are presented in the appendix.

Variable-Stability Airplane

For the flight portion of the present study the 367-80 four-engined jet transport 707 prototype was made available by the Boeing Company under Contract No. NAS 2-2132. The airplane (fig. 3) was adapted for variable-stability test work by the installation of an irreversible rudder servo

system with $\pm 10^{\circ}$ of variable-stability authority. The yawing-moment parameters that were varied during the flight program were static directional stability, N_{β}, sideslip-rate damping, $N_{\dot{\beta}}$, yaw due to roll control input, N_{δ_a}, and yaw due to rolling, N_p.

TESTS

Example Airplane

The example airplane used in the simulator study was one of the final versions of the NASA SCAT 16, a variable-sweep supersonic transport design, in the landing configuration (with wing swept 30°). The basic airplane characteristics, based on available wind-tunnel data and supplemented by theoretical estimates, are given in table I. The values shown in the table for C_{l_p} and L_p were set approximately 60 percent greater than the basic values for the SCAT 16 to ensure a short roll time constant (0.3 sec).

Simulator Test Maneuvers

For simulator evaluation of the lateral-directional characteristics of the airplane, tasks were chosen to represent the most critical low-speed operating conditions. The instrument landing approach was selected as the condition upon which to base the study. This condition requires close concentration by the pilot on instrument flying technique and is one of the situations in which good handling qualities are desirable for safe operation.

Figure 4 illustrates the approach geometry reproduced in the simulator. The initial altitude on a 3° glide slope was 600 feet, which placed the simulated airplane approximately 2 miles from the runway threshold. The approaches were performed under instrument conditions (using deviation information derived from a simulated instrument landing system) until visual contact with the runway was obtained at an altitude of 200 feet. From that point, the pilot completed the approach visually to a landing. During some of the approaches, offsets corresponding to a lateral deviation of 170 feet were introduced abruptly in the localizer needle shortly after the airplane started down the glide slope (fig. 4). These offsets were simulated (in effect) by moving the localizer transmitter 170 feet to the right or left of the runway center line. The pilot's task was to correct, on instruments, the offset by executing a sidestep maneuver. After correcting the initial offset properly, the pilot (upon breaking out at 200 ft) found himself offset from the runway center line; thus, before he could land, it was necessary for him to perform a second sidestep maneuver visually. At the nominal approach speed of 130 knots, the time required for each simulator run was about 50 seconds.

The evaluation in the simulator of each combination of airplane variables was based on the following three tasks: First, the pilot familiarized himself in a general way with the airplane dynamics at the approach

speed of 130 knots by performing turn entries and recoveries, roll reversals, steady sideslips, and Dutch-roll oscillations. Second, he made straight-in instrument approaches. Third, he made instrument approaches, but with the lateral offsets described previously. He corrected the offsets by performing sidesteps with roll control alone and also with coordinating rudder.

The sidestep maneuver was selected as a primary evaluation maneuver because it could be performed realistically in the simulator, because it placed an appreciable demand on the pilot for proper phasing of rudder control when coordination was desired, and because the time required to perform it was close to the Dutch-roll oscillation period predicted for the supersonic transport class of airplane at landing approach speeds. Hence, the possibility of coupling with and unduly exciting the Dutch-roll mode was introduced as a significant factor. Detailed analyses of the sidestep maneuver are given in references 6 through 8. Some flight work reported in reference 9 indicated that the minimum time to perform a sidestep maneuver without exceeding reasonable bank angles was about 10 seconds, which was approximately the Dutch-roll period (at 130 knots) of the SCAT 16 used herein as the basic airplane. To uncover any effects of resonant coupling between the sidestep and the Dutch-roll mode, nominal oscillation periods of 10, 7, and 5 seconds were investigated.

The lateral offset of 170 feet referred to was that value which would result from an idealized sidestep maneuver performed at 130 knots with a sinusoidally varying bank angle having a period of 10 seconds and an amplitude of 20°.

Time histories of typical sidestep maneuvers performed with roll control alone at nominal periods of 10 and 5 seconds are presented in figure 5.

Test Variables

The aerodynamic derivatives chosen as the primary variables in the present study were yaw due to rolling, N_p, and yaw due to the pilot's roll control input, N_{δ_a}, the latter expressed in terms of roll control effectiveness as $N_{\delta_a}/L_{\delta_a}$. These derivatives were varied over the ranges indicated in table II. The ranges chosen were approximately those encountered in several NASA SCAT supersonic transport design studies. The values of Dutch-roll period were set at 10, 7, and 5 seconds, and the damping ratio ζ_d was set at approximately 0.15 by adjusting the yaw damping, N_r, (both at $N_p = -0.118$). The variations of period and damping ratio with N_p over the range studied are shown in table II.

Some runs were made with the damping ratio increased to approximately 0.25 and 0.40 ($P \approx 10$ sec) and also with roll damping L_p reduced to approximately one-third the base value (resulting in a single-degree-of-freedom roll time constant of about 1 sec). These characteristics are summarized in table III.

After completing the evaluation tasks described earlier, the pilot assigned a numerical rating to each combination of variables according to

the scale presented in table IV. (See also ref. 10.) Ratings and pilot's comments were obtained separately for maneuvers performed first without, then with coordinating rudder. Two NASA research pilots participated in the study; however, both pilots did not evaluate all configurations.

Flight Tests

The flight maneuvers performed in the Boeing 367-80 variable-stability jet transport were as follows: (A) Dutch-roll oscillations, aileron step inputs, 5° and 30° heading changes, and simulated sidestep maneuvers (S-turns); and (b) landing approaches using visual reference, then repeated using instrument reference. In the instrument approaches guidance information was supplied by either a deviation indicator or a flight director. Lateral offsets were corrected visually prior to landing. The pilots rated each task according to table IV and assigned an overall rating to each configuration. They used the rudder at their discretion and, in assigning their ratings, considered how much turn coordination was required.

RESULTS AND DISCUSSION

Simulator Study

Effects of primary variables.- The results of the simulator study are presented in figure 6 as pilot opinion boundaries on the N_p, $N_{\delta_a}/L_{\delta_a}$ plane for each of the nominal Dutch-roll periods of 10, 7, and 5 seconds. The individual test points are shown with the associated pilot ratings. The boundaries separate areas of satisfactory and unsatisfactory characteristics for normal operation (PR = 3.5), and areas of acceptable and unacceptable characteristics for emergency, or dampers-out, operation (PR = 6.5). The numerical ratings for obtaining these boundaries were either given by one of the two NASA research pilots involved in the simulator study (see table II), or were the average of both pilots' evaluation of the same combination. Furthermore, the ratings were those given when coordinating rudder was used, except when coordination was ineffective or detrimental.

Figure 6 indicates, for each Dutch-roll period, an area of satisfactory combinations of N_p and $N_{\delta_a}/L_{\delta_a}$. These satisfactory areas are oriented diagonally and indicate a "trade off" between the two yaw-coupling parameters; for example, as N_p becomes more positive (tending to yaw into the turn), $N_{\delta_a}/L_{\delta_a}$ must become less positive if the yaw-coupling characteristics are to remain satisfactory. These results indicate that a positive value (within limits) of either or both of these parameters is desirable.

Pilot comments indicated that behavior in sidestep maneuvers was satisfactory when sideslip excursions were near minimum without the use of coordinating rudder. These comments are substantiated in figure 6 by the diagonal long-dashed lines that pass through the satisfactory areas. These lines are loci of zero values of β_1/φ_1, the ratio of the first peak sideslip

to the first peak bank angle as measured from records of the sidestep maneuvers performed without coordinating rudder. The short-dashed lines are loci of $\omega_\varphi/\omega_d = 1.0$. The ratio ω_φ/ω_d was evolved in reference 11 as an indicator of incipient closed-loop lateral-directional instability for roll control with ailerons only for a pilot-airplane combination; that is, with values of ω_φ/ω_d much greater than 1.0, such instability should be expected, especially at low levels of Dutch-roll damping. The ranges of ω_φ/ω_d in the present study will be discussed in a later section.

In each part of figure 6 the two dashed lines agree well and, furthermore, intersect the vertical axis ($N_{\delta_a}/L_{\delta_a} = 0$) at $N_p \approx g/V$, a condition that, for most airplanes, results in self-coordinating, or two-control, behavior (see, e.g., ref. 12).

The basic value of N_p predicted for the SCAT 16 example was -0.118. In view of the requirements of figure 6 for at least as much positive N_p (with negative or small positive values of $N_{\delta_a}/L_{\delta_a}$), suitable stability augmentation might be desirable if the positive N_p increment cannot be obtained by design modification.

The widening of the satisfactory area at the intermediate Dutch-roll period of 7 seconds (fig. 6(b)) indicates a wider latitude or tolerance of variations of N_p or N_{δ_a}. At first glance, this apparent tolerance might tend to confirm the existence of a resonant coupling effect between the sidestep maneuver and the Dutch-roll mode at the periods of 10 and 5 seconds. The pilot's comments indicated, however, that resonant coupling was virtually undetectable.

To investigate the possibility of resonant coupling, two sets of available quantitative data were examined: (1) measurements of β_1/φ_1 in rudder-fixed sidesteps performed by the pilots during simulator runs, and (2) values of β_1/φ_1 in sidesteps programmed on the analog computer, wherein the simulated airplane was forced to follow closely a sinusoidal bank-angle command having a 10-second period and 10° maximum amplitude. Each set was obtained for several N_p, N_{δ_a} combinations over the test ranges with ζ_d nearly constant at 0.15.

The two sets of data showed very similar trends. The sideslip excursions decreased progressively with decreasing Dutch-roll period (increasing N_β) and there were no peaks or dips in the plotted curves. These measurements substantiate the pilot's comment that coupling between the sidestep maneuver and the Dutch-roll mode was insignificant.

The boundaries of figure 6 have a similarity to those from the piloted simulator study of a V/STOL aircraft in cruising flight (ref. 12).

Effects of yaw and roll damping.- As mentioned earlier, a few configurations were evaluated in the simulator with increased yaw damping, $-N_r$, or decreased roll damping, $-L_p$. The evaluation of these additional configurations by pilot B is summarized in table III. The basic configurations

from table II, identified as points A, B, and C in figure 6, are included. Incremental changes in pilot rating from those for the basic configurations are also shown.

It was expected that increasing the Dutch-roll damping ratio ζ_d above 0.15 would improve handling characteristics in general and that decreasing roll damping (e.g., to about 1/3 the base value) would result in less desirable coupling effects due to an increase in the magnitude of $N_p p$ relative to $N_{\delta_a}\delta_a$ and in the phase difference between roll rate and roll control input.

It is evident from table III that, in one case, the use of yaw-rate damping to improve the damping ratio resulted in only a minor improvement in pilot opinion and, in the other case, a small deterioration in rating. As $-N_r$ was increased, those configurations based on point A ($N_p = -0.20$, $N_{\delta_a}/L_{\delta_a} = 0.005$) benefited somewhat from a decrease in β_1/φ_1, while those configurations based on point B ($N_p = 0$, $N_{\delta_a}/L_{\delta_a} = 0.034$) suffered an increase in β_1/φ_1. The apparent anomaly concerning the effect on β_1/φ_1 of increasing the yaw damping is explained by the fact that although the yaw rate (a contributor to $\dot{\beta}$) decreased with increasing $-N_r$ during sidestep maneuvers in both cases, the increase in $-N_r$ for the configurations based on point B caused a reversal in the phase relationship of the yaw rate to the roll rate, sideslip, and bank angle (the remaining significant contributors to $\dot{\beta}$) and an increase in β_1/φ_1. In both cases, the slight change in numerical pilot rating was about the amount expected from the change in β_1/φ_1 that was measured.

Other studies (e.g., ref. 13) have point out the advantages of using sideslip-rate damping (additional yawing moment proportional to $\dot{\beta}$), and it is believed that applying such a scheme to increase the damping would improve handling qualities as originally expected.

The third group of configurations listed in table III ($P \approx 7$ sec) indicates the effects of decreasing roll damping and, also, of decreasing to zero the distance from the center of gravity to the cockpit.

It is seen that decreasing roll damping to about one-third the base value (τ_R increased from 0.29 to 0.96 sec) did worsen the pilot rating. The ratio ω_φ/ω_d decreased from 0.96 to 0.85, suggesting an increase in adverse sideslip. (Measured β_1/φ_1 increased from 0.16 to 0.20.) Pilot B stated that the combination of $\tau_R = 0.96$ sec, $x_p = 100$ ft, $N_p = -0.118$, and maximum aileron yaw ($N_{\delta_a}/L_{\delta_a} = 0.034$) was very difficult to control with aileron alone in that the Dutch-roll mode was easily excited. Attempts to coordinate with the rudder were of little help.

The final configuration listed in table III was identical to the decreased roll-damping condition just discussed, except that x_p was assumed to be zero. Consequently, somewhat less side-acceleration force at the cockpit should have been evident since sideslip would have been the only contributing factor. Pilot B commented that the accelerations were much milder

and that the contribution due to sideslip seemed very small. Overcontrolling tendencies were lessened. The pilot ratings tend to support this by indicating a slightly smaller deterioration in rating, for $\tau_R = 0.96$, from the basic point C.

Flight Evaluation

To obtain pilot-opinion data in a flight environment for comparison with the simulator results discussed in the previous section, certain combinations of N_p and $N_{\delta_a}/L_{\delta_a}$ were evaluated by NASA pilots A and B in the Boeing 367-80 airplane described earlier. These combinations were selected to represent ranges of variables studied in the simulator and were not intended to provide a point-by-point verification of the simulator results.

Comparison with simulator boundaries.- A comparison of the flight results with the simulator results is presented in figure 7. The bounded areas indicated as satisfactory, unsatisfactory, and unacceptable are from the simulator (repeated from fig. 6) and the plotted points are the flight results.

For the period of 10 seconds (fig. 7(a)), agreement between the flight and simulator ratings was good near the lower unacceptable boundary (PR = 6.5). For the intermediate period of 7 seconds (fig. 7(b)), agreement between simulator and flight data was good only near the lower satisfactory-unsatisfactory boundary (PR = 3.5). For the short period of 5 seconds (fig. 7(c)), the limited flight data show considerable leniency with regard to adverse N_p.

Overall, the flight points in figure 7 show less change in pilot rating with variations of N_p and $N_{\delta_a}/L_{\delta_a}$ than the simulator boundaries indicate. Furthermore, at positive N_p, the flight ratings continued to improve as $N_{\delta_a}/L_{\delta_a}$ was made more positive, even to the limit of the range tested.

The differences between the simulator and flight results in figure 7 indicate that care must be taken in interpreting the results. A possible interpretation is that, with current variable-stability techniques, a conventional jet transport cannot adequately simulate the responses of a configuration such as a supersonic transport. Two fundamental items can influence the quality of the simulation: (1) the differences in geometry between simulator airplane and simulated airplane, and (2) the accuracy with which the stability and control derivatives of the basic simulator airplane are known. The following discussion will attempt to answer the question partially. Some new parameters, which are shown to influence pilot opinion, are introduced. Some attention also is directed toward the effects of airplane geometry.

Variation of pilot rating with β_1/φ_1.- In figure 8, pilot ratings are presented as functions of β_1/φ_1 measured in pedals-fixed sidesteps performed in the simulator and in flight. The simulator data are indicated by the open symbols and the flight points are shown as filled symbols. All pilot rating data fit approximately into two bands which suggest linear variations with β_1/φ_1. For greater positive values of β_1/φ_1, the rate of increase of pilot

rating probably would tend to decrease, since it would be expected that quite high values of β_1/φ_1 could be tolerated without the airplane actually becoming uncontrollable.

The steep rise of numerical pilot rating for negative values of β_1/φ_1 obtained from the simulator data reflects the objectionable characteristics (a tendency toward lateral instability with the pilot in the loop, an impression of greatly decreased roll damping, and a tendency toward spiral divergence) associated with excessive yaw into the turn or with values of ω_φ/ω_d greater than unity. When β_1/φ_1 was negative, coordination with the rudder was undesirable because of the cross-control technique required. Generally, when β_1/φ_1 is positive and less than 0.2, rudder coordination is considered unnecessary.

The similarity in trends of the two sets of data in figure 7 is repeated in the corresponding data of figure 8. Also, the lower sensitivity of pilot rating to changes in N_p and $N_{\delta_a}/L_{\delta_a}$ in flight (fig. 7) is reflected by a lower sensitivity of pilot rating to changes in β_1/φ_1 in flight (fig. 8).

Effect of side accelerations.- The pilots felt that reduced sensitivity of pilot rating to β_1/φ_1 could be attributed to the absence of significant side acceleration forces at the cockpit in flight. In the simulator, these forces included a substantial contribution from yawing angular acceleration acting through the assumed 100-foot cockpit arm and were noticeable, even becoming objectionable for the short period of 5 seconds. Although in establishing their ratings the pilots paid particular attention to the magnitude of the sideslip-angle disturbances in turn entries and reversals, the side acceleration forces experienced in the simulator undoubtedly had a strong adverse effect on their opinions. The above impressions were confirmed by measurements of cockpit side acceleration computed by the analog computer during the simulation and by accelerometer records obtained during the S-turn maneuvers performed in the flight tests.

The results of the above measurements are shown as functions of Dutch-roll period in figure 9 for the values of N_p and $N_{\delta_a}/L_{\delta_a}$ indicated. The results are examined in terms of first-to-second peak sideslip and side-acceleration increments. Although somewhat higher sideslip/bank ratios are noted in flight, the trends with period are similar. The decrease in incremental sideslip for a given bank angle as the period is decreased is expected because of increased static stability. The increase in perceived side acceleration in the simulator with the decrease in period is attributed to the yawing-acceleration component $x_p\dot{r}$ because of the assumed pilot's location far ahead of the center of gravity. The relatively constant side acceleration measured in flight resulted from the much shorter cockpit arm, which allowed the aerodynamic component $Y_\beta\beta$ to be the major contributor.

From these results, it appears that the decreased tolerance of variations in N_p and $N_{\delta_a}/L_{\delta_a}$ at the period of 5 seconds in the simulator was a function of the increased side forces felt by the pilots.

In the flight data, the lack of definition of optimum regions of N_p and N_{δ_a} could have been the result of insufficient coverage of these variables. This, in turn, was probably due to uncertainties in the values and interrelationships of the stability and control derivatives of the unaltered 367-80 airplane.

Correlation with ω_φ/ω_d.- Plots of β_1/φ_1, measured in sidesteps performed without rudder, as a function of ω_φ/ω_d are presented in figure 10 for the cases investigated in the simulator and for the flight-test configurations. The ω_φ/ω_d values were calculated using a digital computer program (not from approximate formulas) with the aerodynamic derivatives and physical characteristics of the airplanes as inputs.

The simulator data show good correlation between the two ratios in that the sideslip excursions were minimal at ω_φ/ω_d near unity (actually, about 1.02) and that a clear relationship can be seen between large positive (adverse) values of β_1/φ_1 and low values of ω_φ/ω_d. The relationship appears to hold for all three values of Dutch-roll period investigated, with very little scatter.

The flight data show a similar relationship; however, somewhat more scatter is evident and zero sideslip excitation appears to correspond to a slightly greater value of ω_φ/ω_d. Sufficient data were not available to show a clear trend for the 5-second period conditions, but the β_1/φ_1 values measured were consistently less than those for the 10- or 7-second period condition.

The pilot-rating data are presented as functions of ω_φ/ω_d in figure 11. It is seen that, in the simulator, the ratings were best near $\omega_\varphi/\omega_d = 1.0$ and deteriorated progressively as ω_φ/ω_d departed from 1.0 in either direction. This variation would be expected from the discussions of figures 6, 8, and 10 and also agrees quite well with the overall trends shown in figure 13 of reference 14.

The flight data in figure 11 indicate generally the same deterioration of ratings for ω_φ/ω_d decreasing below 1.0, but, as mentioned previously, show more scatter. The flight data for ω_φ/ω_d above 1.0 indicate a continued improvement in pilot rating rather than a deterioration. There seems to be no ready explanation for this continued improvement other than the possibility mentioned earlier of uncertainties in the basic aerodynamic derivatives of the 367-80 airplane. ("Effective" values of the variable derivatives were estimated and used in calculating ω_φ and ω_d.)

In general, it appears that either β_1/φ_1 or ω_φ/ω_d, within the ranges of roll damping and Dutch-roll period and damping investigated herein, can serve as a reasonable criterion for assessing the behavior of large transport aircraft in sidesteps and possibly in other types of turning maneuvers. Each parameter has its particular advantages: ω_φ/ω_d has a theoretical basis, but β_1/φ_1 can be measured easily (and therefore demonstrated) in flight in any airplane equipped with sideslip and roll-sensing devices. Some effects of a similar parameter, $\Delta\beta/\Delta\varphi$, on pilot opinion during turn entries are presented

in reference 15. A review of the data from reference 15 and the present study indicates similar variations of pilot rating with some simple measure of peak sideslip per unit maximum bank angle. Uncertainties remain as to the effects of several variables (such as dihedral effect, roll damping, Dutch-roll-damping ratio, and airspeed) on the utility of β_1/φ_1 or $\Delta\beta/\Delta\varphi$ as turn-coordination parameters. Additional research in this area is desirable.

Summary of Pilot Comments

Pilot opinion seemed to be influenced most strongly by the magnitude of the sideslip excursions generated in abrupt, rudder-fixed turn entries and turn reversals. When these excursions were adverse, the improvement realized by use of coordinating rudder was roughly proportional to the amount of sideslip with roll control alone. In the simulator, when sideslip was favorable (β_1/φ_1 negative), the pilots considered the reversed rudder coordination required in turn entries to be unnatural and impractical.

When the sideslip excursions were large and adverse, there was a tendency to excite an oscillation in heading when a small heading change was being made with ailerons alone. This problem appeared to be independent of period and occurred when bank angle was used to control heading. When the desired heading was not achieved, the pilot increased the bank angle. The desired heading change was achieved only with considerable sideslip. As the sideslip returned to zero, the pilot would see that he had overshot and would correct back. In extreme cases during IFR flight, this oscillation could become divergent. The solution to this problem was to apply rudder vigorously. Although this use of rudder control was effective, the resultant increase in the pilot's work load degraded his opinion of the configuration.

In general, the pilots found it difficult to determine which parameter (N_p, N_{δ_a}, or other) was the primary cause of the sideslip excursions. They did observe, however, that the extreme positive values of N_p seemed to reduce the spiral stability of the vehicle. (These statements apply both to the simulator and flight evaluations.)

CONCLUSIONS

A piloted five-degree-of-freedom simulator and a large variable-stability airplane have been used to study the effects of the aerodynamic yaw-coupling parameters on the lateral-directional handling qualities of a supersonic transport at landing-approach speed. From this study, the following conclusions are drawn:

1. Combinations of N_p (yaw due to rolling) and N_{δ_a} (yaw due to roll control application) corresponding approximately to the frequency ratio $\omega_\varphi/\omega_d = 1$ resulted in the most favorable pilot opinions because they required

minimum rudder coordination in turn entries and reversals. In some cases, these combinations included positive values of both parameters.

2. For the supersonic transport configuration represented in the simulator, the values of N_p required for optimum yaw coupling generally were positive (i.e., less adverse than usual for N_p at lift coefficients attained in the landing approach).

3. The amount of departure from optimum values of the yaw-coupling derivatives (especially N_p) that could be tolerated in the positive direction was less than that in the negative (adverse) direction because of incipient closed-loop lateral-directional instability (pilot controlling) and the airplane's tendency to diverge spirally.

4. The magnitude of sideslip excursions in sidesteps, for a given combination of N_p and $N_{\delta_a}/L_{\delta_a}$, was related mainly to the static directional stability N_β, and there was apparently no magnification, or resonance effect, due to coupling with the Dutch-roll mode at the nominal periods of 10 and 5 seconds.

5. In the simulator, ω_φ/ω_d correlated well with the sideslip-to-bank ratio β_1/φ_1 measured in pedals-fixed sidestep maneuvers. In flight, the correlation was somewhat less consistent.

6. In the simulator, both ω_φ/ω_d and β_1/φ_1 correlated well with numerical pilot rating. The ratio β_1/φ_1 is easily measured in flight and may have application as a criterion for satisfactory or acceptable yaw-coupling characteristics in turning maneuvers. Values of β_1/φ_1 between 0 and 0.2 were considered sufficiently small to require no coordination with rudder.

Ames Research Center
National Aeronautics and Space Administration
Moffett Field, Calif., 94035, Sept. 2, 1966
720-04-00-01-00-21

APPENDIX

AIRPLANE EQUATIONS OF MOTION AND ANGULAR CONVERSIONS

The following equations of motion were mechanized by means of a general-purpose electronic analog computer. The moment equations were written in the body system of axes and the force equations were referred to wind axes. The effects of the product of inertia I_{XZ} were assumed to be negligible.

BASIC MOTION EQUATIONS

Linear Accelerations

$$\dot{V} = \frac{T}{m} - \frac{V^2 \rho S}{2m} C_D - g\gamma$$

$$a_Y = \frac{V^2 \rho S}{2m} (C_{Y_\beta} + C_D)\ \beta - \frac{T}{m}\beta + g \sin \varphi$$

$$a_Z = -\frac{V^2 \rho S}{2m} (C_{L_\alpha}\alpha + C_{L_{\delta_e}}\delta_e) - \frac{T}{m}\alpha + g \cos \varphi$$

Angular Accelerations

$$\dot{q} = \frac{V^2 \rho S \bar{c}}{2I_Y} (C_{m_\alpha}\alpha + C_{m_{\delta_e}}\delta_e) + \frac{V \rho S \bar{c}^2}{4I_Y} C_{m_q} q - \frac{I_X - I_Z}{I_Y} pr$$

$$\dot{p} = \frac{V^2 \rho S b}{2I_X} (C_{l_\beta}\beta + C_{l_{\delta_a}}\delta_a + C_{l_{\delta_r}}\delta_r) + \frac{V \rho S b^2}{4I_X} (C_{l_p} p + C_{l_r} r)$$

$$\dot{r} = \frac{V^2 \rho S b}{2I_Z} (C_{n_\beta}\beta + C_{n_{\delta_a}}\delta_a + C_{n_{\delta_r}}\delta_r) + \frac{V \rho S b^2}{4I_Z} (C_{n_p} p + C_{n_r} r) - \frac{I_Y - I_X}{I_Z} pq$$

RELATIVE WIND

$$\alpha = \int \dot{\alpha}\, dt = \int \left(\frac{a_Z}{V} + q - p\beta \right) dt$$

$$\beta = \int \dot{\beta}\, dt = \int \left(\frac{a_Y}{V} - r + p\alpha \right) dt$$

EULER ANGLES

$$\theta = \gamma + \alpha + \beta \sin \varphi$$

$$\varphi = \int \dot{\varphi}\, dt = \int \left(p + r\alpha - \frac{a_Z}{V} \beta \right) dt$$

$$\psi = \lambda - \beta + \alpha \sin \varphi$$

FLIGHT PATH

$$\lambda = \int \dot{\lambda}\, dt = \int \left(\frac{a_Y}{V} \cos \varphi - \frac{a_Z}{V} \sin \varphi \right) dt$$

$$\gamma = \int \dot{\gamma}\, dt = \int \left(- \frac{a_Z}{V} \cos \varphi - \frac{a_Y}{V} \sin \varphi \right) dt$$

$$h = \int \dot{h}\, dt = \int V\gamma\, dt$$

REFERENCES

1. McNeill, Walter E.; and Innis, Robert C.: A Simulator Study of the Lateral-Directional Handling Qualities of Two SCAT Configurations in the Landing Approach. NASA TM X-905, 1963.

2. Stapleford, Robert L.; Johnson, Donald E.; Teper, Gary L.; and Weir, David H.: Development of Satisfactory Lateral-Directional Handling Qualities in the Landing Approach. NASA CR 239, July 1965 (Prepared under Contract NAS2-864 by Systems Technology, Inc., Hawthorne, Calif.).

3. McNeill, Walter E.; and Innis, Robert C.: The Effect of Yaw Coupling in Turning Maneuvers of Large Transport Aircraft. NASA SP-83, 1965.

4. White, Maurice D.; Vomaske, Richard F.; McNeill, Walter E.; and Cooper, George E.: A Preliminary Study of Handling Qualities Requirements of Supersonic Transports in High-Speed Cruising Flight Using Piloted Simulators. NASA TN D-1888, 1963.

5. McNeill, Walter E.: A Piloted Simulator Study of the Loss of Altitude by a Jet Transport in a Go-Around From an Instrument Landing Approach. NASA TN D-2060, 1963.

6. Etkin, B.: An Analytical Study of the Ability of a Slender Delta-Wing Aeroplane to Perform a Sidestep Manoeuvre at Low Speed. R.A.E. TN Aero. 2623, 1959.

7. Pinsker, W. J. G.: Further Consideration of the Control Requirements for a Slender Delta Aircraft to Perform Sidestep Manoeuvres at Approach Speeds. R.A.E. TN Aero. 2735, 1961.

8. Tomlinson, B. N.: An Extensive Theoretical Study of the Ability of Slender-Wing Aircraft to Perform Sidestep Manoeuvres at Approach Speeds. R.A.E. TN Aero. 2837, 1962.

9. Perry, D. H.; Port, W. G. A.; and Morrall, J. C.: A Flight Study of the Sidestep Manoeuvre During Landing. R.A.E. Rep. Aero. 2654, 1961.

10. Cooper, George E.: Understanding and Interpreting Pilot Opinion. Aeron. Eng. Rev., vol. 16, no. 3, Mar. 1957, pp. 47-51, 56.

11. Ashkenas, Irving L.; and McRuer, Duane T.: The Determination of Lateral Handling Quality Requirements from Airframe - Human Pilot System Studies. WADC Tech. Rep. 59-135, June 1959.

12. Dolbin, Benjamin H., Jr.; and Eckhart, Franklin F.: Investigation of Lateral-Directional Handling Qualities of V/STOL Airplanes in Cruising Flight. Cornell Aero. Lab. Rep. TB-1794-F-3 (Contract No. P.O. 78839-CAP), Dec. 15, 1963.

13. Quigley, Hervey C.; and Lawson, Herbert F., Jr.: Simulator Study of the Lateral-Directional Handling Qualities of a Large Four-Propellered STOL Transport Airplane. NASA TN D-1773, 1963.

14. Ashkenas, Irving L.: A Study of Conventional Airplane Handling Qualities Requirements; Part II.- Lateral-Directional Oscillatory Handling Qualities. AFFDL-TR-65-138, Nov. 1965.

15. Quigley, Hervey C.; Vomaske, Richard F.; and Innis, Robert C.: Lateral-Directional Augmentation Criteria for Jet Swept-Wing Transport Airplanes Operating at STOL Airspeeds. NASA SP-116, 1966.

TABLE I.- AERODYNAMIC AND PHYSICAL CHARACTERISTICS OF THE BASIC SIMULATED AIRPLANE

[All aerodynamic coefficients are based on wing geometry at 75° sweep angle]

Parameter	Value	Parameter	Value
C_{n_β}	0.2030	$\bar{c}$	63.26
C_{n_p}	-0.5525	Λ_{LE}(landing	
C_{n_r}	-0.6284	configuration)	30°
$^1C_{n_{\delta_a}}$	-0.00595	ρ	0.002378
$C_{n_{\delta_r}}$	-0.0811	W	252,400
C_{l_β}	-0.1806	V	220
C_{l_p}	-2.713	ϵ	0.5°
C_{l_r}	0.9746	N_β	0.255
$^1C_{l_{\delta_a}}$	-0.1940	N_p	-0.1176
$C_{l_{\delta_r}}$	0.0158	N_r	-0.1337
C_{Y_β}	-0.478	$^1N_{\delta_a}$	-0.0075
C_{m_α}	-0.264	N_{δ_r}	-0.102
C_{m_q}	-1.382	L_β	-1.357
$C_{m_{\delta_e}}$	-0.710	L_p	-3.443
C_{L_α}	3.52	L_r	1.238
$C_{L_{\delta_e}}$	0.66	$^1L_{\delta_a}$	-1.457
C_L	1.083	L_{δ_r}	0.119
I_X	2.24×10^6	Y_β	-13.99
I_Y	11.54×10^6	Control limit	
I_Z	13.37×10^6		
I_{XZ}	9.9×10^4	δ_r	±25°
α_{trim}	4.0°	$^2\delta_a$	±15°
S	4000	δ_e	-20°, 10°
b	74.30		

[1]Both ailerons deflected; referred to total aileron angle.

[2]Single aileron.

TABLE II.- PRINCIPAL COMBINATIONS OF AERODYNAMIC DERIVATIVES CONSIDERED AND PILOT RATINGS OBTAINED IN THE PRESENT STUDY

$[\zeta_d \approx 0.15, -\frac{1}{L_p} = 0.29]$

N_β	N_r	N_p	$\frac{N_{\delta_a}}{L_{\delta_a}}$	P	ζ_d	$\frac{\lvert\varphi\rvert}{\lvert\beta\rvert}$	$\frac{\omega_\varphi}{\omega_d}$	Pilot rating			
								Pilot A		Pilot B	
								No rudder	Using rudder	No rudder	Using rudder
(a) Nominal period, 10 sec											
		-0.20	0.005	9.9	0.15	0.69	0.81	7-1/2	7	7	6
		-.20	.017	9.9	.15	.69	.83	8	7-1/2		
		-.20	.034	9.9	.15	.69	.86	7	6-1/2		
		-.118	.005	10.3	.15	.72	.84	7-1/2	6-1/2		
0.255	-0.054	0	-.034	11.1	.14	.77	.81	8	7		
		0	.005	11.1	.14	.77	.91	6	5-1/2		
		0	.034	11.1	.14	.77	.98	3	---	3	2-3/4
		.10	.034	11.9	.13	.82	1.05	4-1/2	4-1/2		
		.20	-.034	13.0	.12	.88	.95	4-1/2	4-1/2		
		.20	-.017	13.0	.12	.88	1.00	3-1/2	3-1/2	3-1/2	3-3/4
		.20	.005	13.0	.12	.88	1.07	4	5		
		.20	.034	13.0	.12	.88	1.15	6	6	6	6
(b) Nominal period, 7 sec											
		-.20	.005	6.9	.17	.54	.90			6-1/2	5-3/4
		-.20	.034	6.9	.17	.54	.93	6-1/2	5		
		-.118	.034	7.1	.16	.55	.96			5-1/2	5
		0	-.034	7.3	.15	.56	.92			6	5
		0	.005	7.3	.15	.56	.96	4	3-1/2		
		0	.017	7.3	.15	.56	.97	4	3-1/2		
.668	-.152	0	.034	7.3	.15	.56	.99			3-1/4	3
		.10	-.017	7.5	.14	.57	.97			4-1/2	3-3/4
		.10	.005	7.5	.14	.57	.99	3	3		
		.10	.017	7.5	.14	.57	1.00			2-1/2	2-1/2
		.10	.034	7.5	.14	.57	1.02	3	3		
		.20	-.034	7.8	.13	.59	.99	4	3-1/2		
		.20	-.017	7.8	.13	.59	1.00			3	3
		.20	.005	7.8	.13	.59	1.03	3	3		
		.20	.034	7.8	.13	.59	1.06			4-1/2	4-1/2
(c) Nominal period, 5 sec											
		-.20	.005	4.9	.15	.45	.95			6	5
		-.20	.034	4.9	.15	.45	.96			5	4-3/4
		-.118	.005	5.0	.15	.45	.96			5	4-1/2
		0	-.034	5.1	.14	.46	.96			6	5
1.448	-.230	0	.005	5.1	.14	.46	.98			4	4
		0	.034	5.1	.14	.46	.99	2	---	3	3
		.10	.034	5.2	.13	.46	1.01			3-3/4	4
		.20	-.034	5.3	.13	.47	1.00			4-1/4	3-1/2
		.20	-.017	5.3	.13	.47	1.00			4	3-1/2
		.20	.005	5.3	.13	.47	1.01			4	4
		.20	.034	5.3	.13	.47	1.03	4	4	4-1/4	4-1/4

TABLE III.- EFFECTS OF THE SECONDARY VARIABLES N_r, τ_R, AND x_p

Nominal period, sec	Basic point (fig. 6)	N_β	N_r	N_p	$\frac{N_{\delta a}}{L_{\delta a}}$	τ_R	x_p	P	ζ_d	$\frac{\lvert\varphi\rvert}{\lvert\beta\rvert}$	$\frac{\omega_\varphi}{\omega_d}$	$\frac{\beta_1}{\varphi_1}$	Pilot rating (Pilot B)		ΔPR
													No rudder	Using rudder	
10	A	0.255	-0.054	-0.20	0.005	0.29	100	9.9	0.15	0.69	0.81	0.54	7	6	---
		.255	-.248	-.20	.005	.29	100	10.1	.28	.65	.82	.48	7	6	0
		.255	-.440	-.20	.005	.29	100	10.6	.41	.61	.84	.45	6-1/2	5-1/2	-1/2
	B	.255	-.054	0	.034	.29	100	11.1	.14	.77	.98	.10	3	2-3/4	---
		.255	-.220	0	.034	.29	100	11.2	.25	.73	.98	.13	3	---	0
		.255	-.385	0	.034	.29	100	11.7	.37	.69	1.00	.19	3-1/2	3-1/2	3/4
7	C	.668	-.152	-.118	.034	.29	100	7.1	.16	.55	.96	.16	5-1/2	5	---
		.668	-.152	-.118	.034	.96	100	6.3	.10	1.22	.85	.20	7	6-1/2	1-1/2
		.668	-.152	-.118	.034	.96	0	6.3	.10	1.22	.85	.23	6-1/2	5-3/4	3/4

TABLE IV.- PILOTS' RATING SCHEDULE[1]

	Adjective rating	Numerical rating	Description	Primary mission accomplished	Can be landed
Normal operation	Satisfactory	1	Excellent, includes optimum	Yes	Yes
		2	Good, pleasant to fly	Yes	Yes
		3	Satisfactory, but with some mildly unpleasant characteristics	Yes	Yes
Emergency operation	Unsatisfactory	4	Acceptable, but with unpleasant characteristics	Yes	Yes
		5	Unacceptable for normal operation	Doubtful	Yes
		6	Acceptable for emergency condition only	Doubtful	Yes
No operation	Unacceptable	7	Unacceptable even for emergency condition	No	Doubtful
		8	Unacceptable - dangerous	No	No
		9	Unacceptable - uncontrollable	No	No
	Catastrophic	10	Motions possibly violent enough to prevent pilot escape	No	No

[1]In the present study the primary mission was to complete an ILS approach. The ratings were influenced mainly by the most difficult portion of the approach task, which usually was the sidestep maneuver under IFR conditions. The ability to land was not considered explicitly in rating a configuration, but formed a part of the whole task.

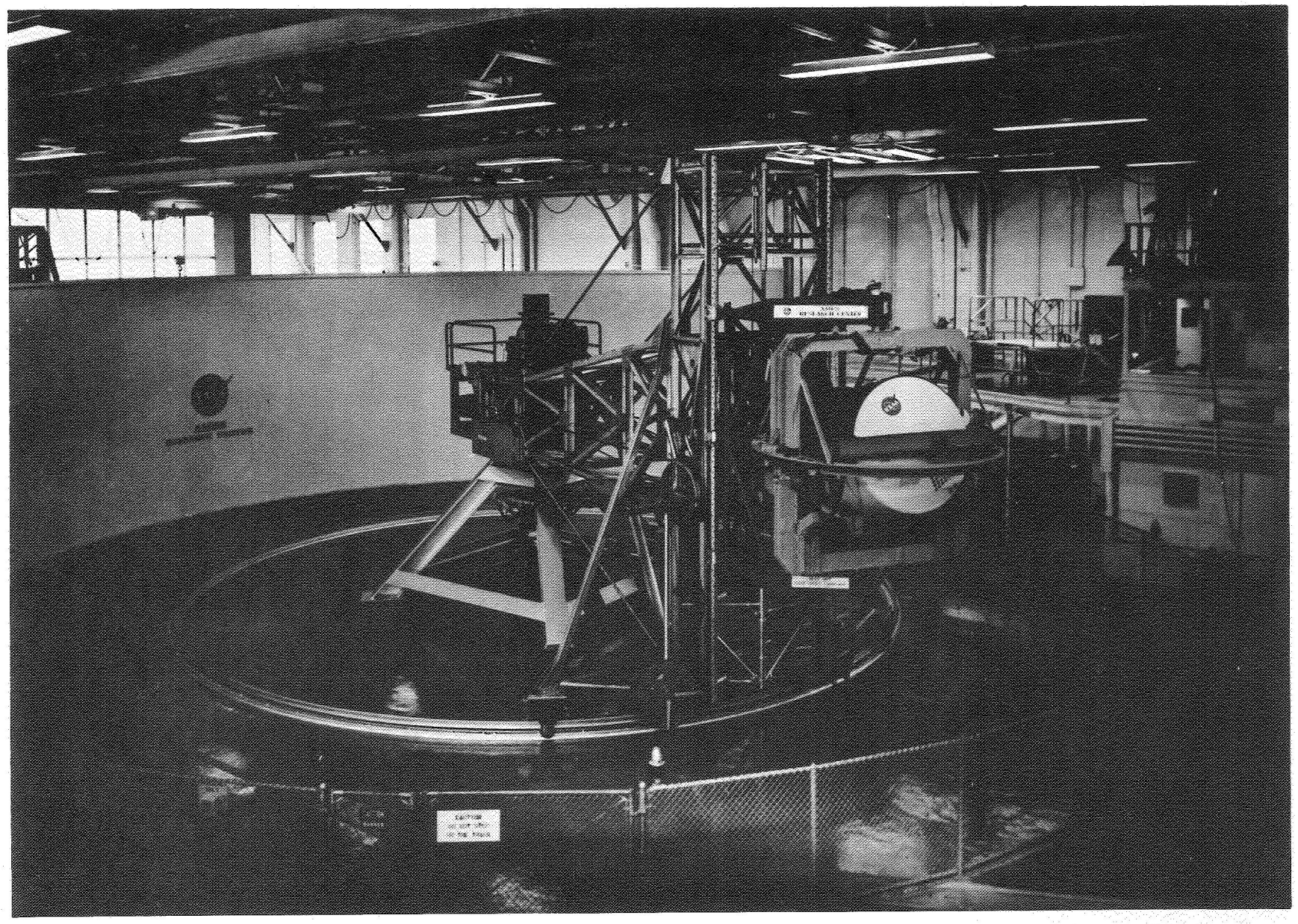

A-31542

Figure 1.- Motion simulator used in the present study.

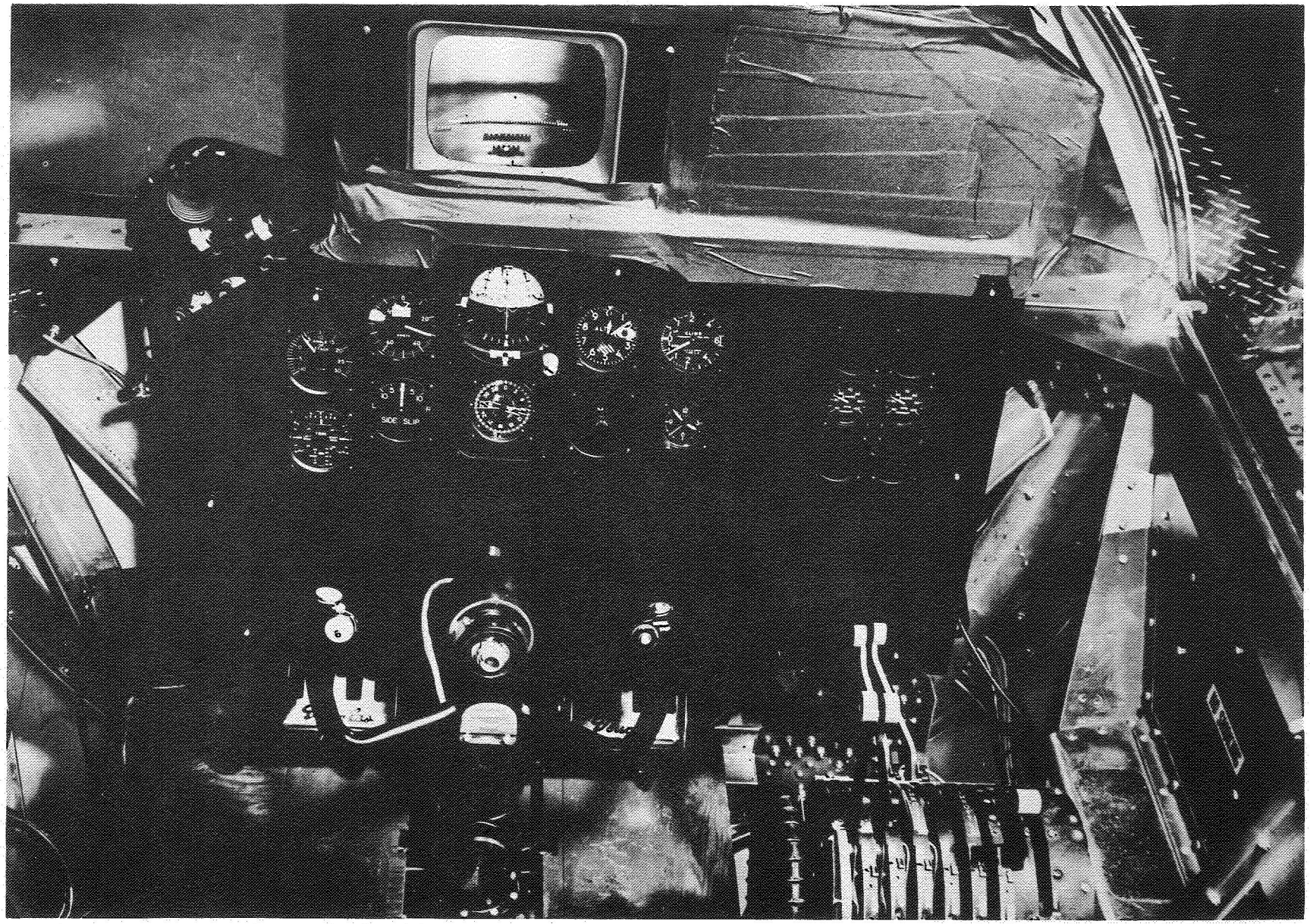

A-32049

Figure 2.- Simulator cockpit interior, including controls, instruments, and visual display.

A-37324

Figure 3.- Variable-stability jet transport used in the flight evaluation.

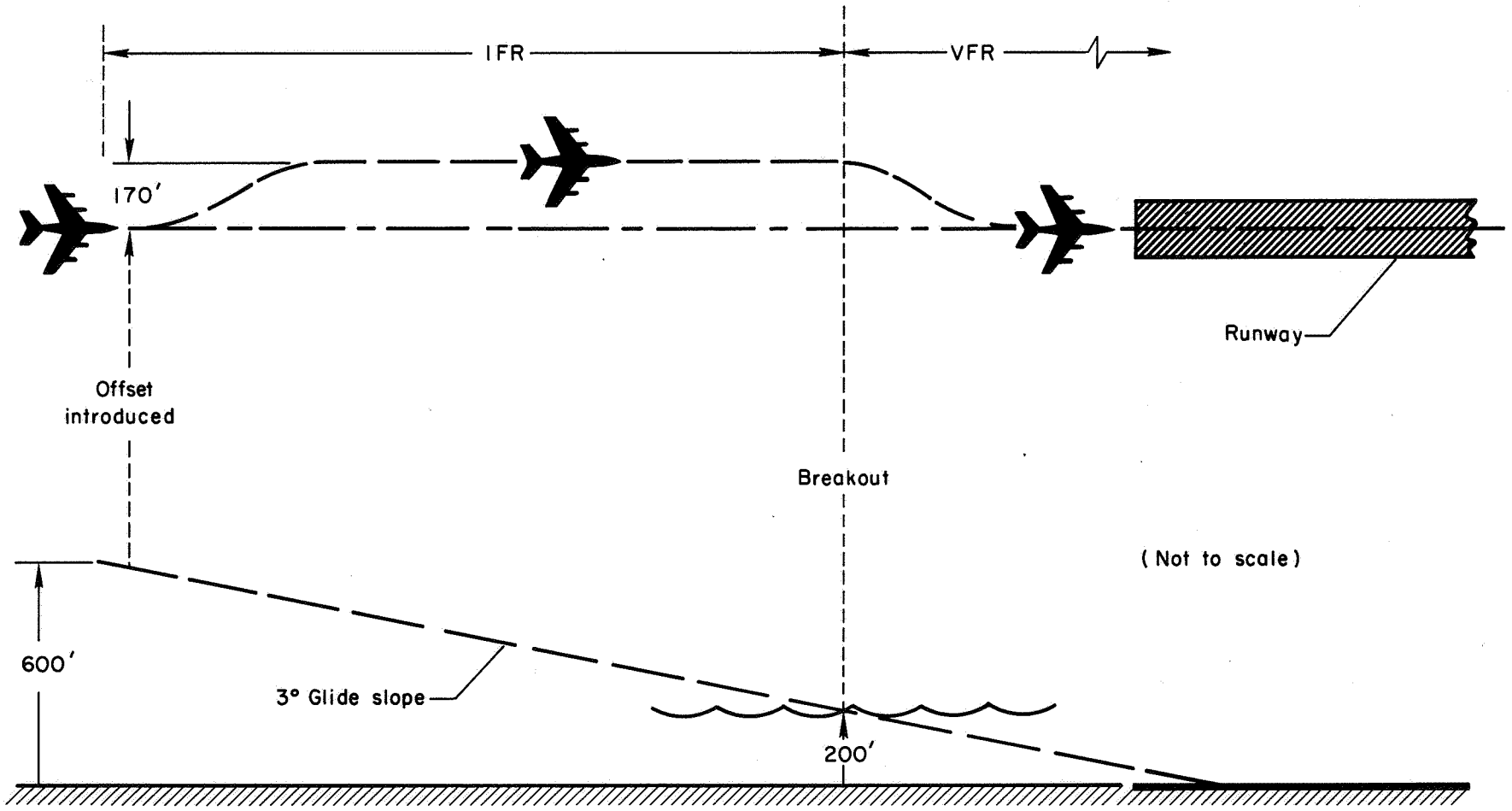

Figure 4.- Schematic drawing of the offset correction task used in the simulator.

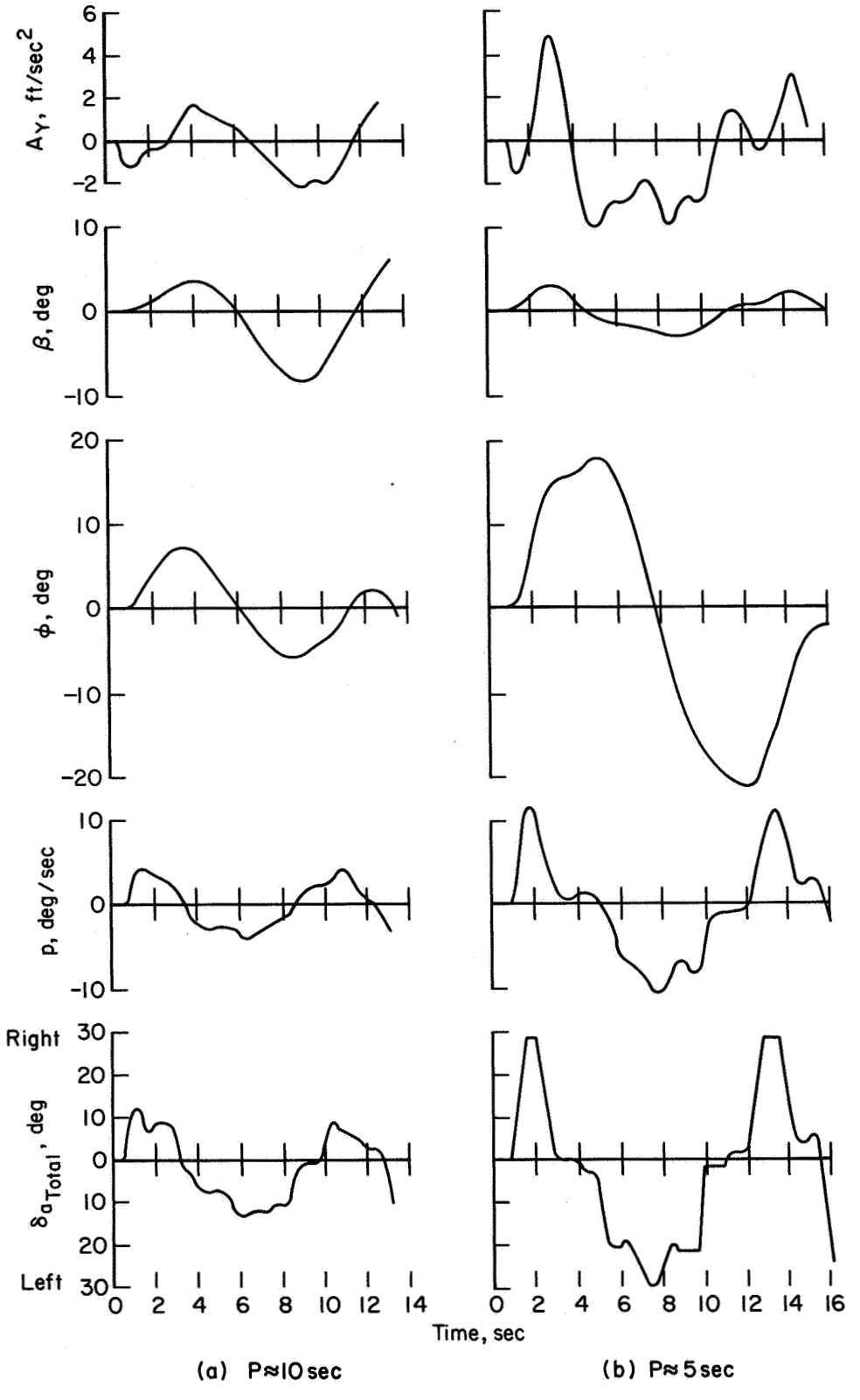

Figure 5.- Time histories of sidesteps performed in the simulator with aileron alone; $N_p = -0.20$, $N_{\delta_a}/L_{\delta_a} = 0.005$.

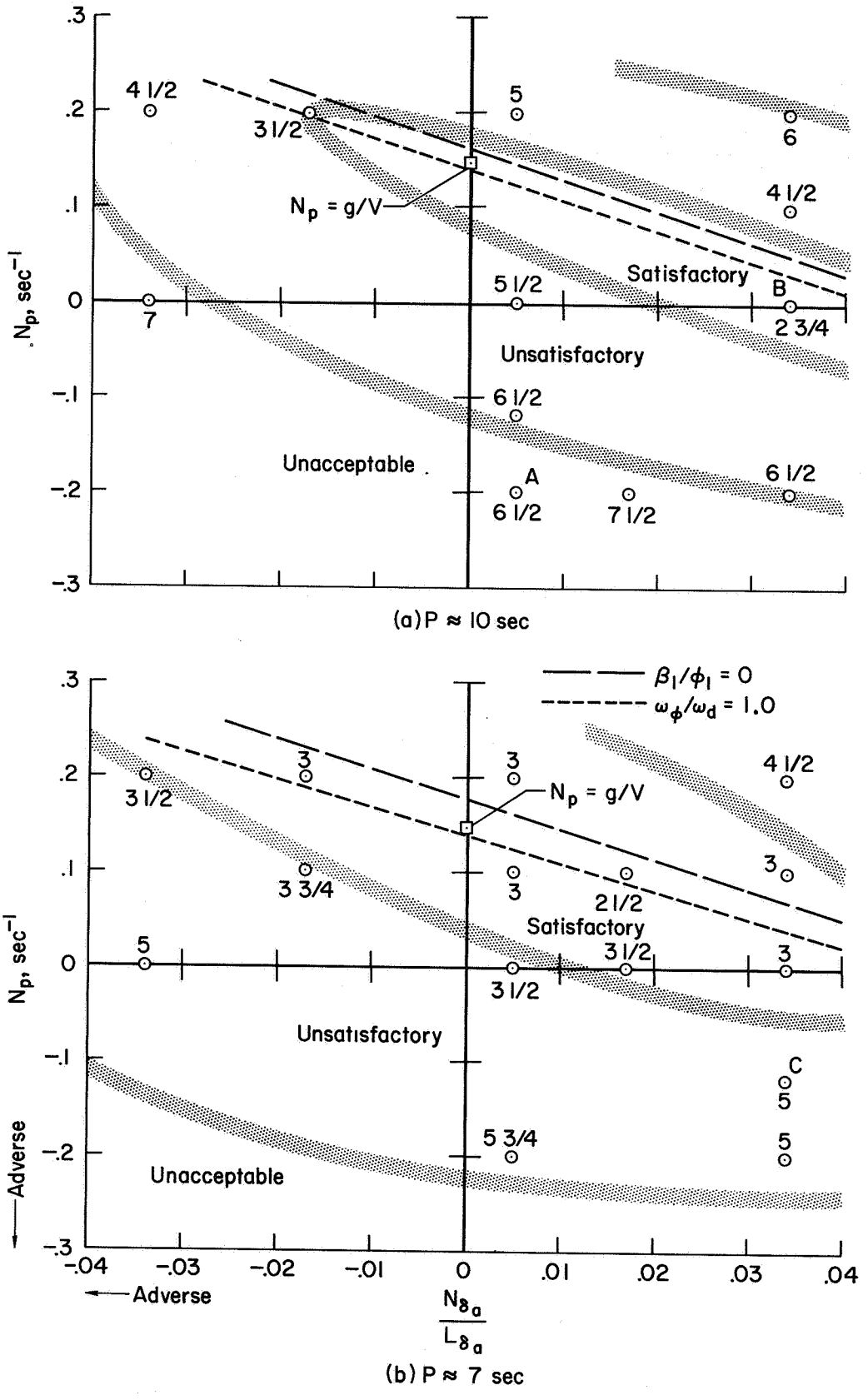

Figure 6.- Simulator data points and pilot-opinion boundaries.

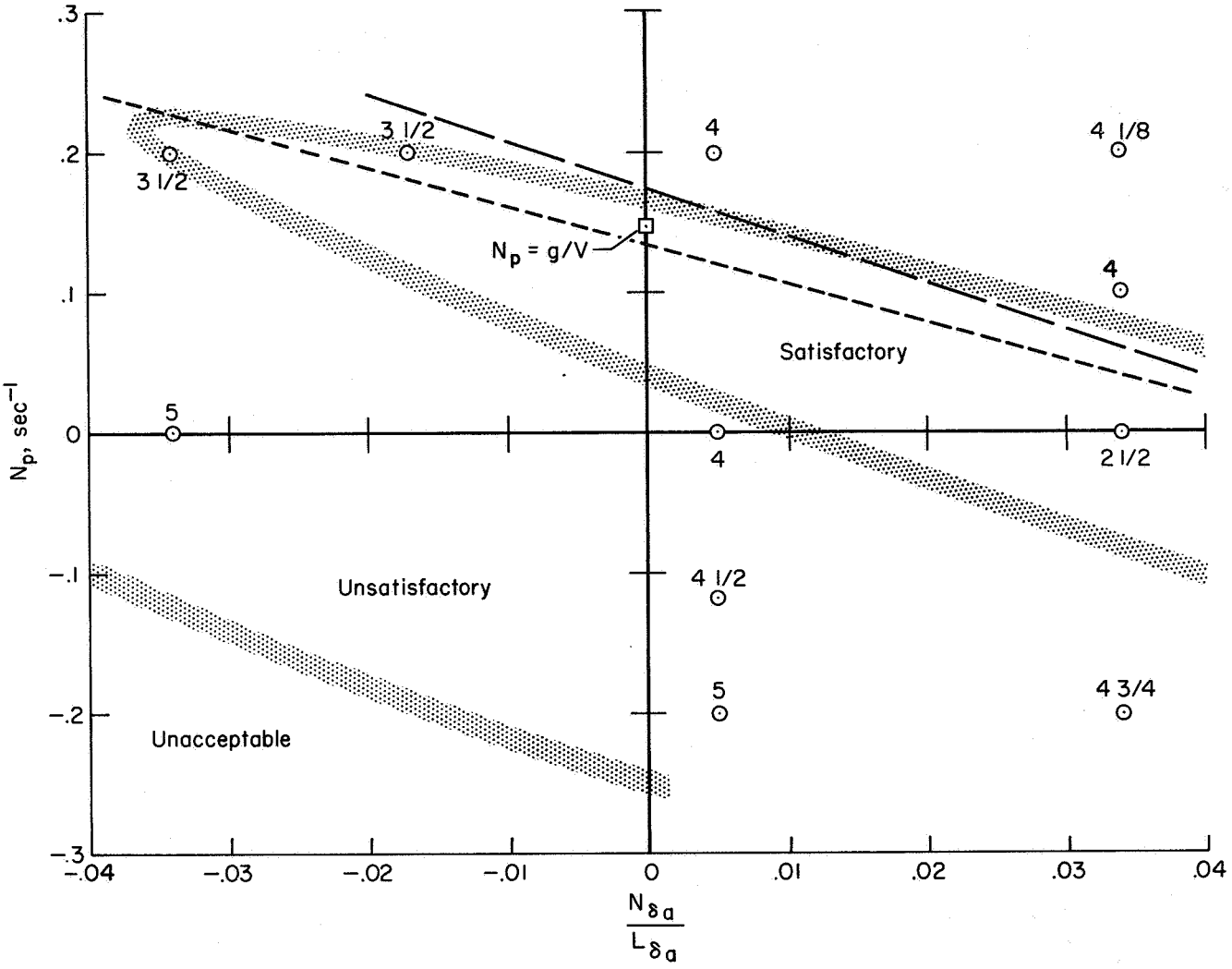

(c) $P \approx 5$ sec

Figure 6.- Concluded.

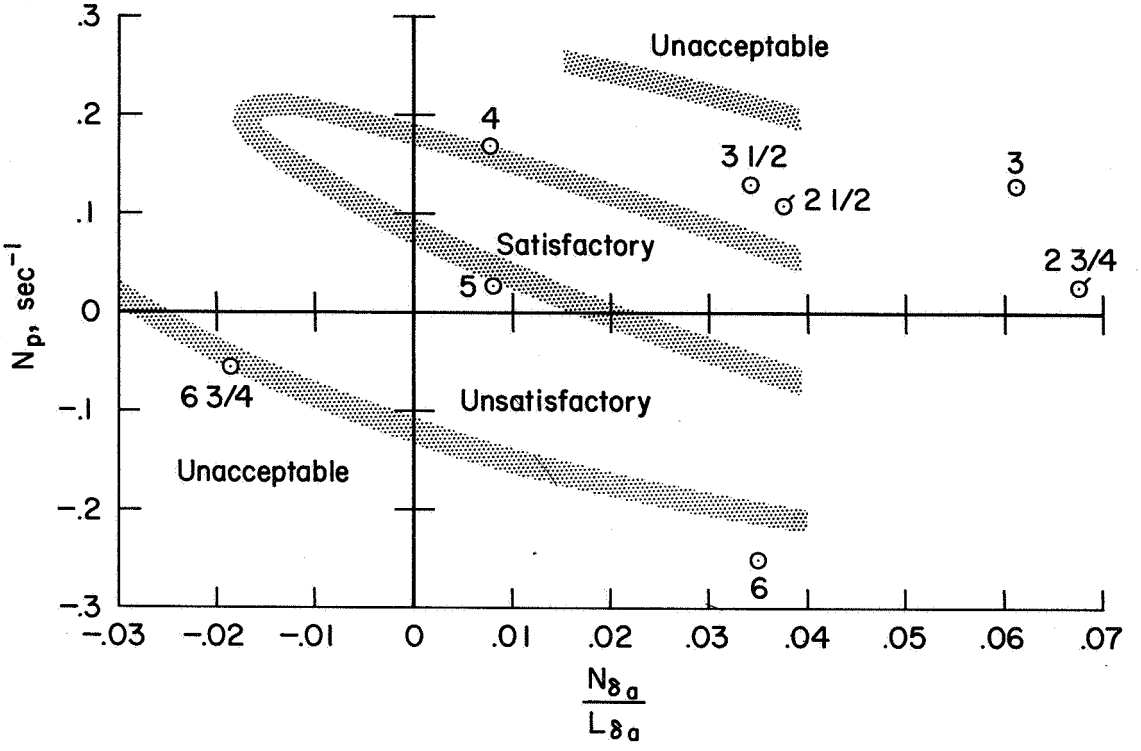

(a) P ≈ 10 sec

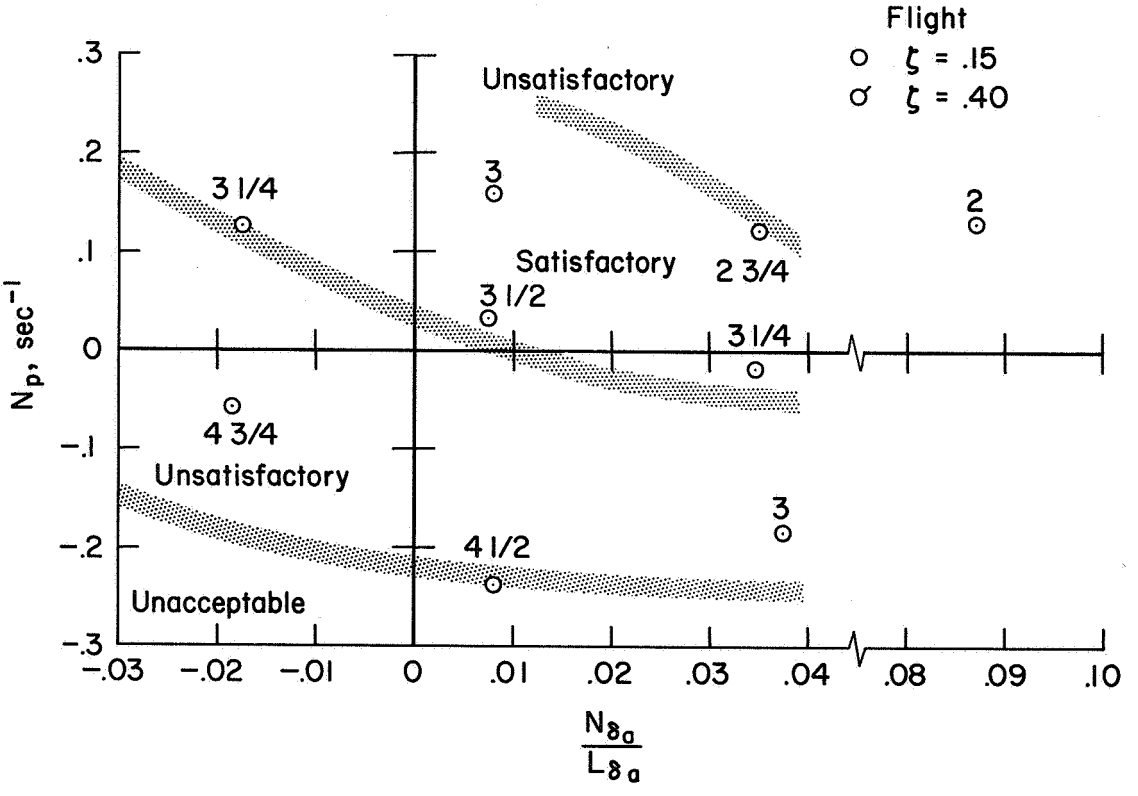

(b) P ≈ 7 sec

Figure 7.- Comparison of pilot ratings obtained in flight with opinion boundaries obtained from simulator data.

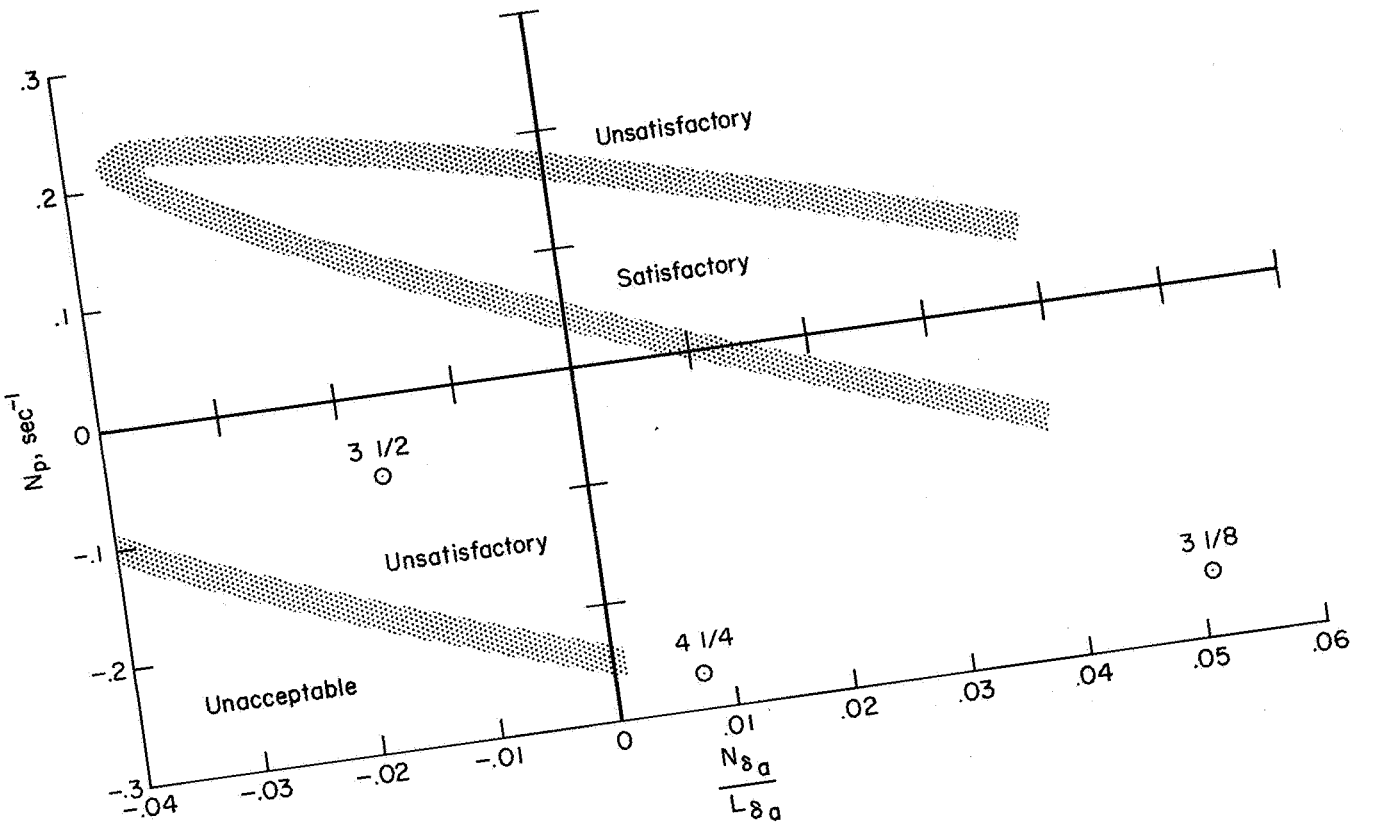

(c) $P \approx 5$ sec

Figure 7.- Concluded.

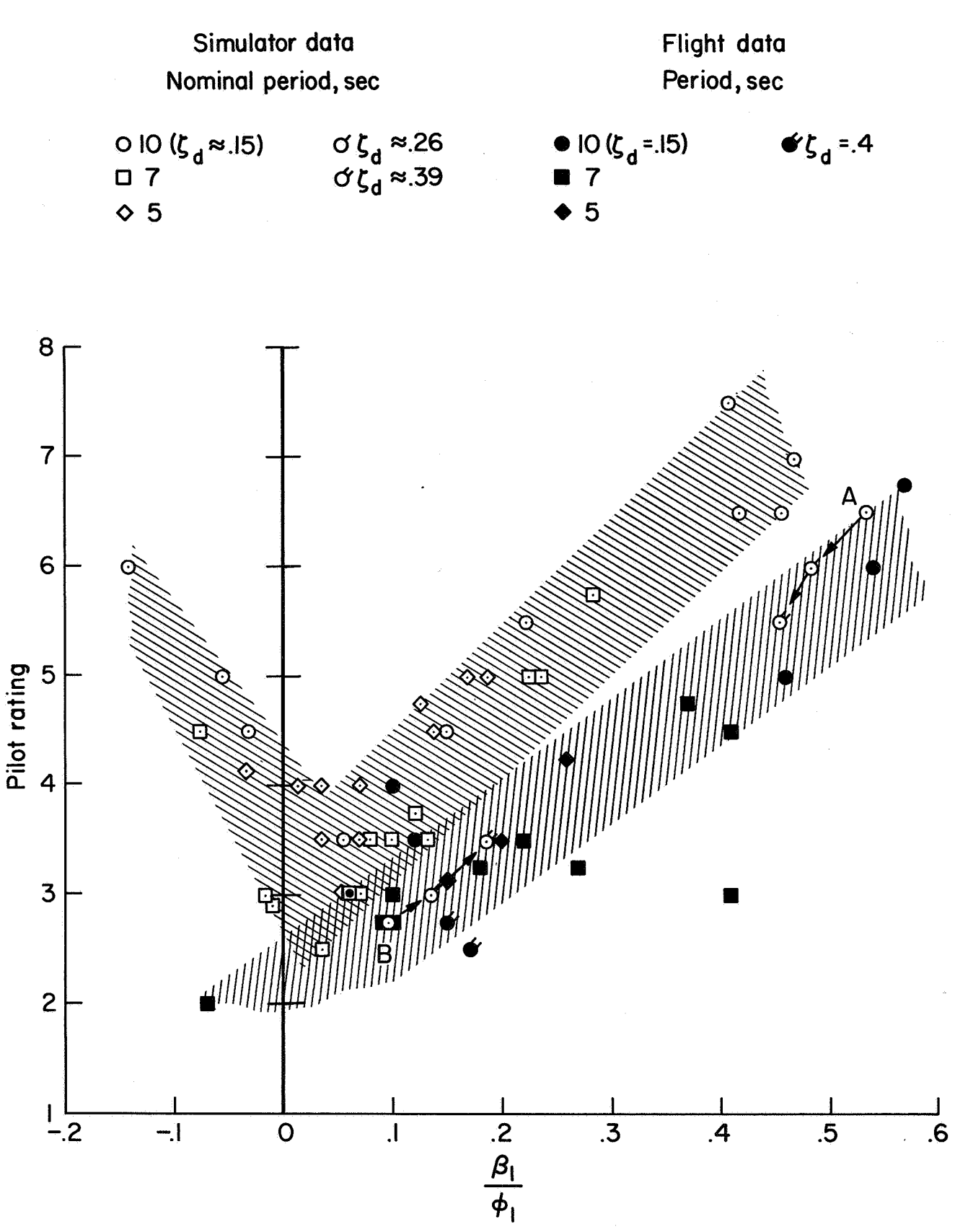

Figure 8.- Variation of pilot rating with the first peak sideslip/bank ratio for simulator and flight data.

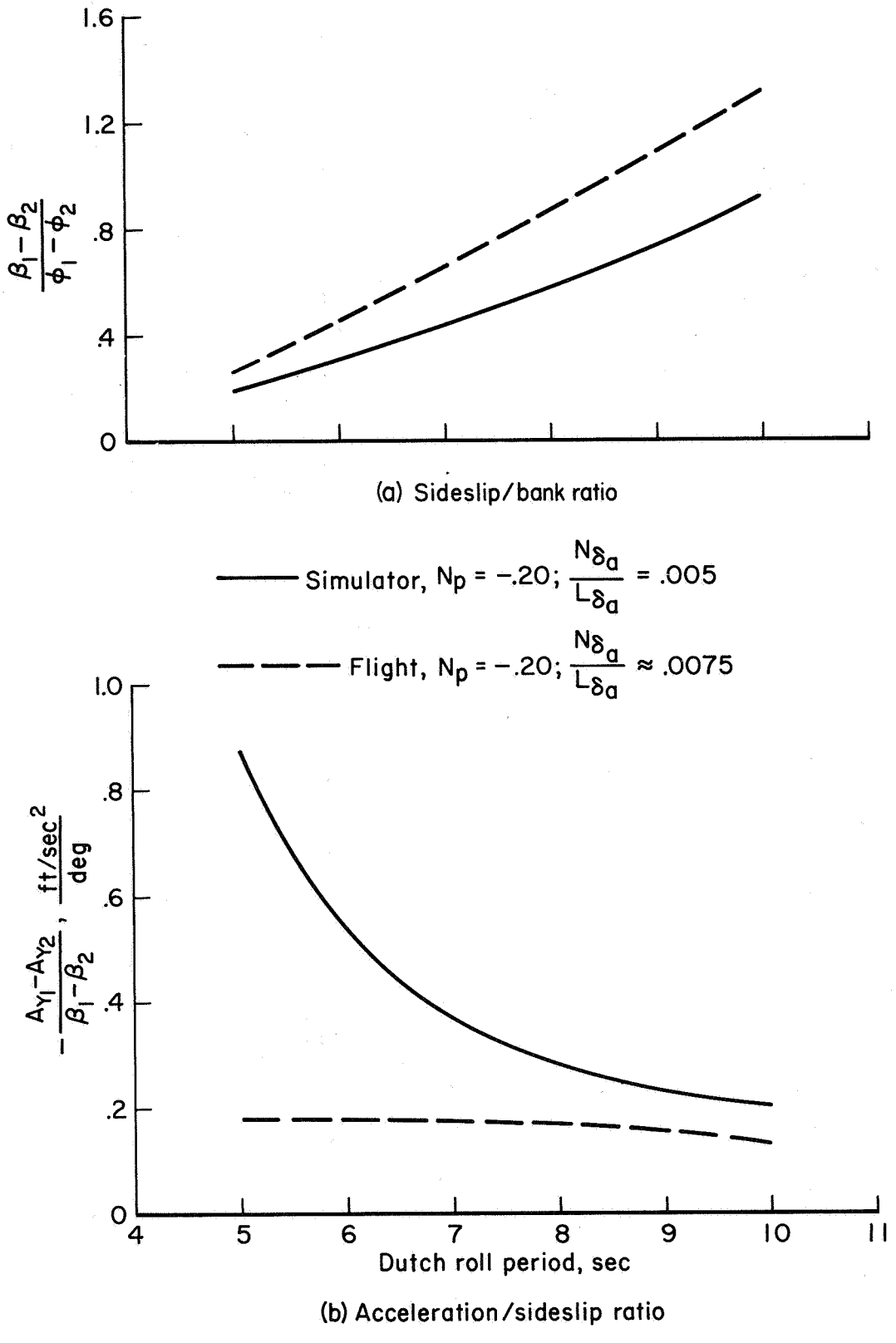

Figure 9.- Variation of sideslip and side-acceleration parameters with period. Rudder pedals fixed; $\zeta_d = 0.15$.

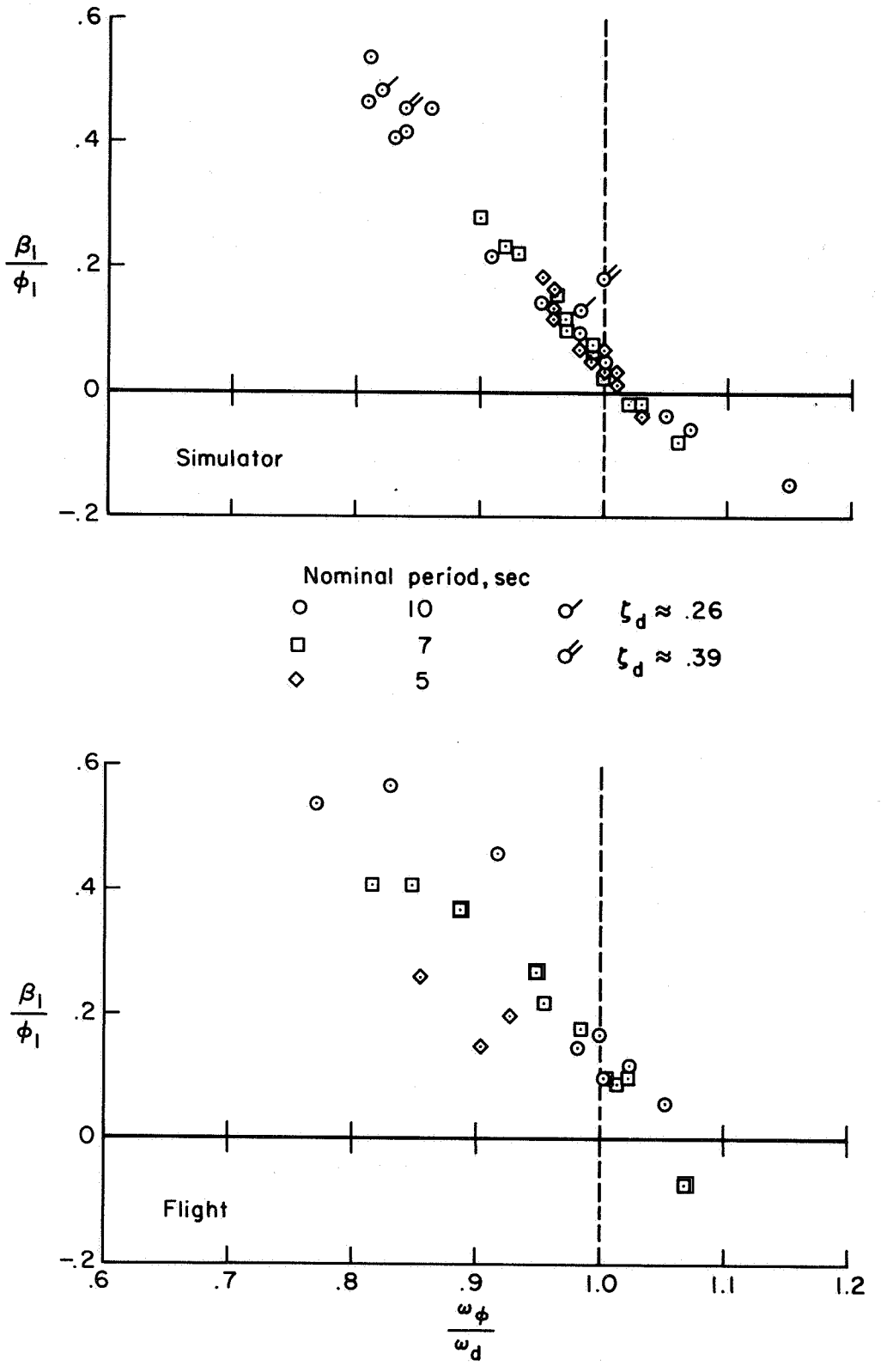

Figure 10.- Variation of the first peak sideslip/bank ratio with ω_φ/ω_d for simulator and flight data.

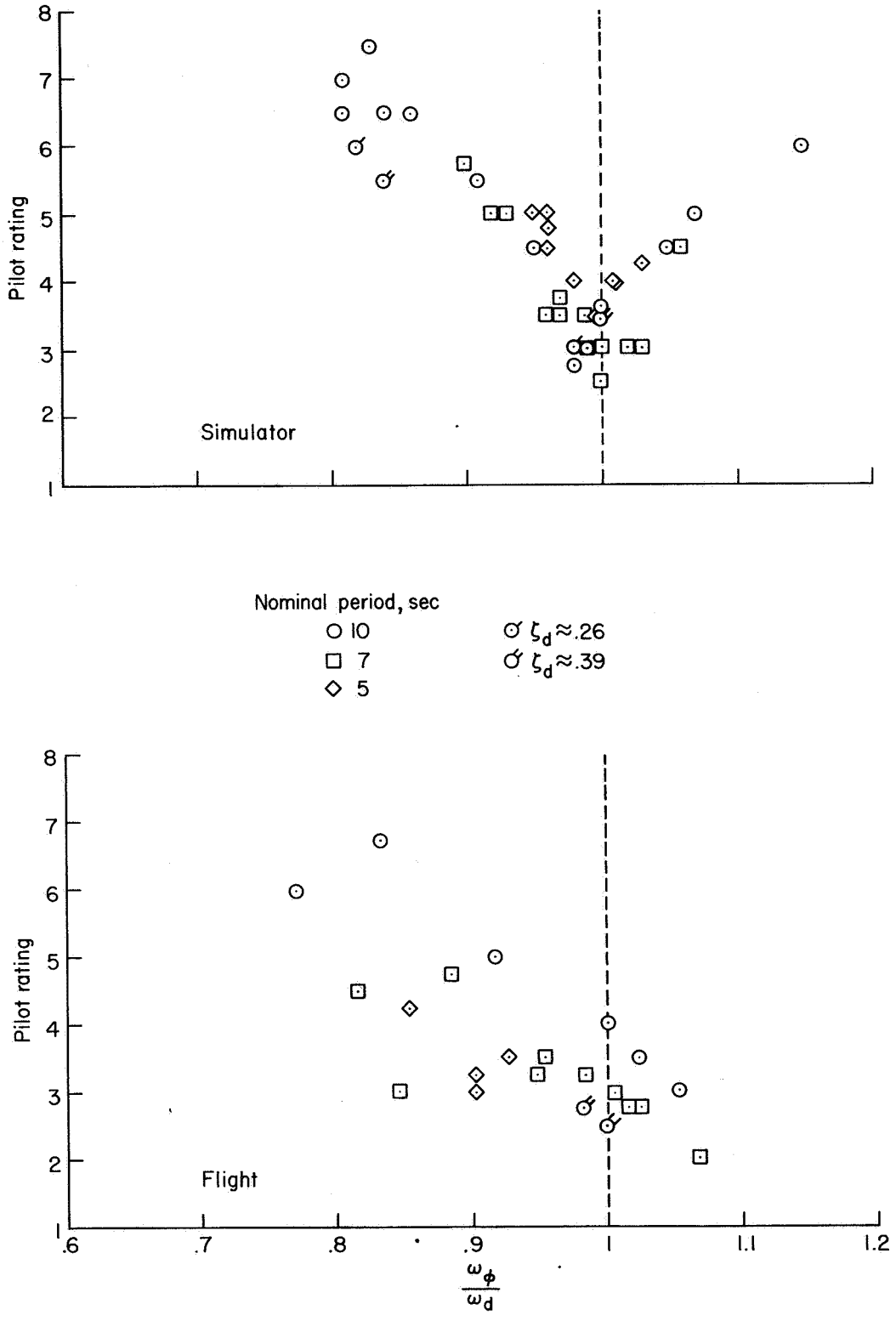

Figure 11.- Variation of pilot rating with ω_φ/ω_d for simulator and flight data.